THE DEVELOPMENT OF PREFERRED ORIENTATION IN Ni-Mo-Al-X AND Ni-Cr-Al-X SUPERALLOYS

H. A. Chin* and A. M. Adair**

*Pratt and Whitney Aircraft EDFO
West Palm Beach, FL 33402

**AFWAL Materials Laboratory
WPAFB, Ohio 45433

Summary

The development of preferred crystallographic orientation was studied in advanced nickel based superalloys of the type Ni-Mo-Al-X*** and Ni-Cr-Al-X***. Principal variables of interest were mode of deformation (e.g. extrusion, rolling), deformation temperature and reduction, and effect of initial texture. Textures developed in the Ni-Mo-Al-X alloys were typical of moderately high stacking fault energy (SFE) face centered cubic (FCC) metals, whilst textures for the Ni-Cr-Al-X alloy were typical of low SFE-FCC alloys.

Introduction

Despite the large production of nickel based superalloys for gas turbine application, no fundamental study of superalloy crystallographic texture and its control by thermomechanical processing has been addressed in the literature. Yet, it is recognized that preferred crystal orientation (texture) is one of the principal factors for optimizing specific properties. The gas turbine module is especially dependent on improvements of such properties as high temperature creep capability, stability and environmental resistance. Alloys currently being used in the turbine module were developed more than 15 years ago due to the inability to overcome conventional casting and fabrication techniques.

Superalloy powder metallurgy studies at Pratt & Whitney Aircraft/ Engineering Division-Florida Operation (EDFO) have shown that powders solidified at very high cooling rates can minimize those constraints (1-5). More effective alloying was therefore achieved and resulted in the development of advanced nickel based blade and vane superalloys of the type Ni-Mo-Al-X and Ni-Cr-Al-X respectively. These alloys exhibited improved high temperature properties over the best available production airfoil material. While this program has not been fully completed, the work has progressed to a point sufficient to demonstrate a workable scheme for those turbine components. Processing schemes involve consolidation of the alloy powder, selective processing to develop specific crystallographic textures in a given product shape and solid state directional recrystallization (DR) to

***X represents single or combined additions of W, Ta, Ti, C, B, Zr.

a single crystal. Orientation of the DR crystals was found to be strongly dependent on the texture of the polycrystals. An extensive study was therefore undertaken to characterize texture development as a function of thermomechanical processing schedule and represents the substance of this paper.

The alloy compositions studied are listed in Table I, of which alloys 185 and 116 are the "base" Ni-Mo-Al-X and Ni-Cr-Al-X alloys respectively. Both base alloys are FCC γ matrix phase with a high volume fraction of coherent ordered FCC γ' -Ni_3Al phase. Modification to the alloys-X involved W, Ta, Ti, C, B, Zr. These alloys were produced by rapid solidification by PWA/GPD rotary atomization and forced convective cooling with helium under inert conditions (1-5). Spherical powder particles in the 10-100 micron range were produced.

Experimental Procedure

Rapidly solidified powders were placed in stainless steel cans immediately after hot dynamic outgassing at 1000°F and 10^{-5} torr pressure. Rectangular (rolling bloom) cans were used for hot isostatic pressing (HIP) and cylindrical cans for extrusion. Powders were then subjected to extensive consolidation and subsequent rolling per the processing flow chart indicated in Figure 1. Principal variables of interest were mode of deformation (e.g. extrusion, rolling, etc.), deformation temperature and reduction, and the effect of initial texture.

HIP was performed at 2250°F/2 hr./15 ksi pressure. Extrusion parameters investigated are listed in Table II. These parameters were chosen from earlier unpublished studies. Hot rolling was conducted on the canned alloys using a reduction per pass schedule of 5% to start with a gradual increase to 20% as rolling progressed. Rolling parameters are indicated in Table III.

Cold rolling studies were conducted on either HIP, extruded or hot rolled alloy. Reductions per pass were of the order $\sim$1%. Intermediate anneals were performed every 5-10% reduction for 5 minutes at 2200°F. Cold cross rolling was also investigated and accomplished as either an intermediate or final portion of the rolling schedule. Cross rolling parameters are listed in Table IV.

X-ray diffraction methods involving an automated goniometer system were used to determine the crystallographic texture of the processed alloys. Plotting of the pole figures were accomplished using a PDP computer and software written by Love (6).

Results

HIP

The subsolvus HIP parameters were found to affect full consolidation of the powder billet. Pole figure analysis of the HIP product revealed a random distribution of crystal orientations or non-textured condition in both alloys.

Extrusion

For the extrusion parameters used, full consolidation of the powder billet resulted. Pole figure analysis of the extruded products revealed

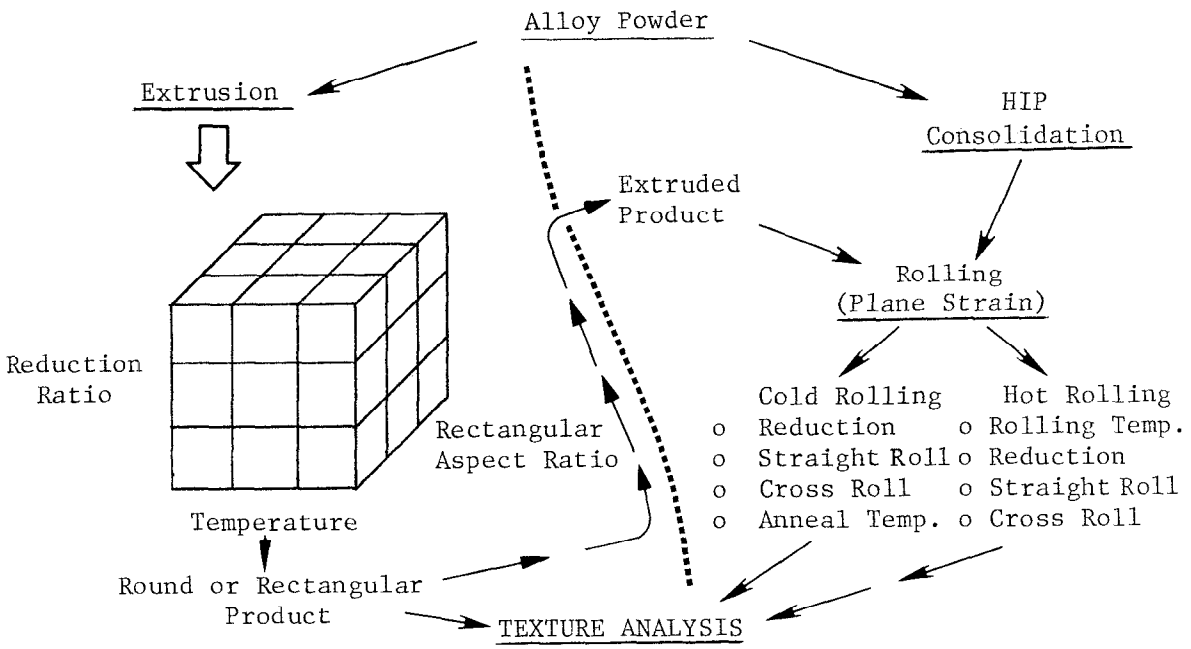

Figure 1. Flow Chart of Thermomechanical Processing For Rapidly Solidified Ni-Mo-Al-X and Ni-Cr-Al-X Alloys

Table I. List of Alloy Compositions Studied

	Composition w/o						
Alloy	Ni	Mo	Cr	Al	W	Ta	Other
185	bal.	14.4	-	6.8	6.25		A
116	bal.	-	9.2	8.3	9.4		A
211	bal.	13.0	-	7.3	6.2		
240	bal.	12.9	-	6.3	3.0	3.0	A
398	bal.	-	14.3	5.8	-	6.0	B
462	bal.	12.3	-	8.08	6.3		
467	bal.	13.0	6.0	7.3	6.25		
469	bal.	9.15	-	8.18	6.38		
605	bal.	11.5	-	6.8	6.3		C
606	bal.	11.5	3.0	6.6	6.3	1.5	
607	bal.	10.0	-	6.6	6.0		C
608	bal.	12.3	-	8.2	6.2		
X	bal.	10.0	3.0	6.8	6.0	1.5	
505	bal.	-	8.9	6.95	9.5	3.11	
512	bal.	1.0	9.01	7.01	9.56	1.57	D
609	bal.	1.0	9.0	7.0	9.5	3.0	
610	bal.	1.0	5.0	7.0	9.5		
XR75	bal.	1.0	8.96	7.0	9.5	1.56	E
Y	bal.	1.0	8.8	6.75	9.7	3.07	F

A - C-0.04
B - C-0.04, Zr-0.04
C - C-0.04, B-0.01, Zr-0.04
D - Ti- 1.25
E - Cb-0.8, C-0.05, B-0.01, Zr-0.1
F - C-0.004

Table II. List of Extrusion Parameters for Rapidly Solidified Ni-Mo-Al-X and Ni-Cr-Al-X Alloys

	EXTRUSION		PRODUCT
Alloy	Temp. °F	Reduction Ratio	Aspect Ratio *
185	2300	43:1, 30:1, 25:1 15:1, 10:1, 8:1	Round
185	2250, 2200, 2100	30:1, 25:1, 15:1, 8:1	Round
185	2050	30:1	Round
185	2000	30:1, 15:1, 8:1	Round
185	1900	8:1	Round
116	2300, 2250	30:1, 25:1, 15:1, 8:1	Round
116	2200, 2100	30:1, 25:1, 15:1, 8:1	Round
116	2000	23:1	Round
116	1900	15:1, 8:1	Round
185	2300, 2200, 2100	25:1	4:1, 3:1, 2:1, 1:1
185	2200	15:1	4:1, 3:1, 2:1
185	2200	10:1	4:1
116	2300	25:1	4:1
116	2200, 2000	25:1	4:1, 3:1, 2:1, 1:1
116	2200	15:1	2:1
116	2200	10:1	4:1
116	2100	25:1	4:1, 3:1, 2:1
116	1900	10:1	4:1
XR75, 609, 610, 605, 606, 607 608	2250	15:1	4:1
398	2300, 2200	25:1	Round
505	2300	15:1	4:1
512, 211	2300	17:1	4:1
467	2300	25:1	4:1
Y	2275, 2250	12:1	3:1, 2.5:1, 2:1
240, 467	2300	15:1	Round

*Width:Thickness ratio of Rectangular Product

Table III. List of HOT Rolling Parameters for Ni-Mo-Al-X and Ni-Cr-Al-X Alloys

Alloy	Rolling Temperature °F	Total Reduction
185	2275	90
185	2250	78
185	2100	75
185	2000	84
116	2250, 2100	75
X,Y	2250, 2200	70

that the two classes of alloys, Ni-Mo-Al-X (185) and Ni-Cr-Al-X (116) developed extrusion textures typical of moderately high and low stacking fault energy FCC metals, respectively (7, 8). In cases where the Mo content of the base alloy 185 was lowered to <10 wt%, and the Cr content in alloy 116 lowered to <5%, a texture transition was observed.

TABLE IV. List of Cold Rolling Parameters for Ni-Mo-X and Ni-Cr-Al-X Alloys

Alloy	Initial ** Condition	Rolling Temperature, °F	SR:XR * Ratio	Total Reduction, %
185	A	RT	SR Only	15,25,35,55
185	B	RT	SR Only	18,31,56,76,90
X,Y	C	RT	SR Only	15,25,35,55
211	A	RT	SR Only	75
462	A	RT	SR Only	73.3
474	A	RT	SR Only	76
185	A,B, or C	RT	60:40	73,78,85
185	A,B, or C	RT	70:30	73
185	A,B, or C	RT	75:25	67,78,85
185	A,B, or C	RT	80:20	73,78
185	A,B, or C	RT	34:48:18	71
185	A,B, or C	RT	42:42:16	71
185	A,B, or C	RT	60:25:15	71
116	A,B, or C	RT	65:35,75:25	67
185	A,B, or C	2200	60:40	80
185	A,B, or C	2100	70:30	91
185	A,B, or C	2000	50:50	84
116	A,B, or C	2300	65:35	91
605,606	A,B, or C	RT	75:25	70
607,608	A,B, or C	RT	75:25	70
X	A,B, or C	RT	80:20 75:25,70:30	60,80
Y	A,B, or C	RT	75:25	62

*A - Extrusion, B - HIP billets, C - HIP + hot roll
**Straight Roll/Cross Roll

Axisymmetric Extrusions. Alloy 185 (Ni-Mo-Al-X) developed four different textural conditions, depending on the processing temperature and reduction. Table V gives a partial listing of representative results which are illustrated in Figure 2. Alloy 116 developed two textural conditions and is also detailed in Table V and Figure 2. For the limited processing matrix studied with the modified Ni-Mo-Al-X alloys 240, 467, 606 and 608, and modified Ni-Cr-Al-X alloy 398, the textures developed were generic to the base compositions. The range of textures produced in both classes of

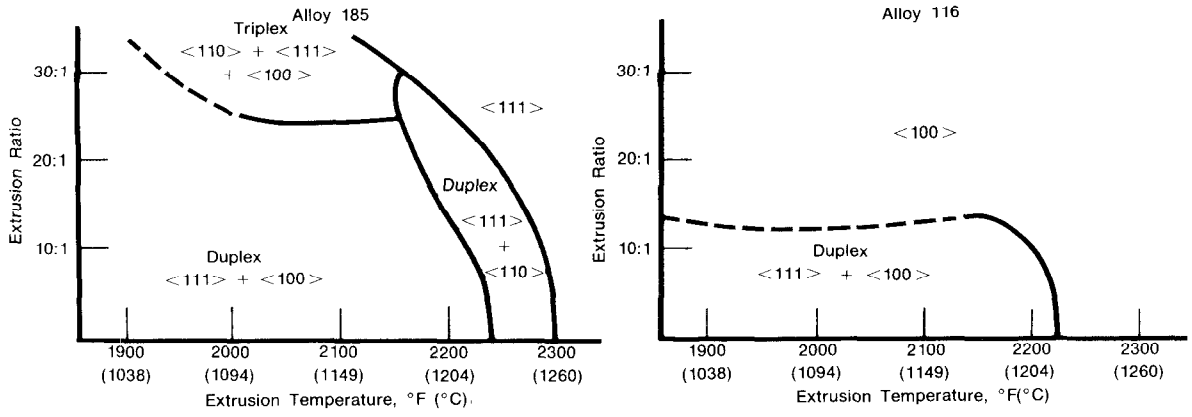

Figure 2. Fiber Textures in Alloys 185 and 116 as Influenced by Extrusion Ratio and Temperature.

Table V. Partial List of Axisymmetric Extrusion Parameters and Resulting Textures

Alloy	Temperature, °F	Extrusion Ratio	Fiber Texture Components
185	2000	15:1	<100>, <111> weak
185	2100	25:1	<100>, <110>, <111> weak
185	2250	15:1	<110>, <111> weak
185	2300	26:1	<111> weak
116	2100	15:1	<100> strong, <111> weak
116	2250	8:1	<100> strong
116	1900	8:1	<100>, <111> weak
240	2300	15:1	<111> weak
467	2300	15:1	<111> moderate
606	2300	15:1	<111> weak
608	2300	15:1	<111> weak
398	2300	20:1	<100> strong
398	2200	20:1	<100> moderately strong

alloys followed the changes expected in FCC alloys from varying stacking fault energy (SFE) and processing temperatures. The high temperature extrusions of both alloys appeared to occur above the γ' solvus (as single phase γ) due to adiabatic heating during deformation. Under this condition, alloy 185 exhibited the singular <111> fiber texture typical of higher SFE FCC alloys undergoing a temperature related texture transition. Alloy 116 exhibited a singular <100> fiber texture typical of a low SFE FCC alloy. Lowering the processing temperature in both alloys resulted in a texture transition to the commonly observed duplex <111> + <100> fiber texture for the moderate-to-low SFE FCC alloys. The existance of the <110> fiber component found in alloy 185 processed in the intermediate temperature range has not been reported in the literature for FCC metals. The development of that texture component is not understood at this time and requires further investigation.

Rectangular Extrusions. For rectangular extrusions, the alloys were observed to develop a sheet type texture, i.e. preferred crystal orientation in the three principal rectangular directions. The perfection of the sheet texture was observed to increase with the width:thickness ratio of the rectangular product, as the deformation transformed from "axisymmetric" 1:1 ratio to plane strain deformation at 2.5:1 ratio. At 1:1 ratio, fiber textures were produced. At 2:1 and 2.5:1 ratios, a weakly defined sheet texture {110}<001> was developed. At 3.1 ratio, the sheet texture was fully defined, see Figure 3 for Alloy Y (Ni-Cr-Al-X).

Textures developed in Alloy 116 (Ni-Cr-Al-X) and its modifications were moderate to strong, exhibiting intensities up to 15 times random. On the other hand, Alloy 185 (Ni-Mo-Al-X) and its modifications exhibited textural strengths ranging from essentially random to 2-3 times random. Such behavior suggests fundamental differences in the recrystallization behavior of both classes of alloys and is thought to be related to the stacking fault energy. McQueen and Jonas (9) reported on other alloy systems with high stacking fault energy which, when subjected to high temperature/strain deformation, undergo dynamic recovery followed by static recovery and recrystallization; on the other hand, metals with low SFE undergo both dynamic recovery and recrystallization followed by static recovery and recrystallization. How the difference affects the texture strength is not fully understood at this time and further studies are ongoing.

Table VI. Partial List of Representative Textures Developed in Ni-Mo-Al-X and Ni-Cr-Al-X 3:1 or 4:1 Aspect Ratio Rectangular Extrusions.

Alloy	Extrusion Temperature, °F	Reduction Ratio	Texture
185	2300	25:1, 15:1, 10:1	{110}<011>
185	2200, 2100	10:1	Spread {110}<110> to {100}<011>
211	2300	17:1	{110}<011>
605, 606, 608	2250	15:1	{110}<011>
467	2250	25:1	{110}<011>
607, 609, XR75	2250	15:1	{110}<011>
116, 505	2300	25:1	{110}<001>
116	2100	25:1	Spread {110}<001> to {100}<001>
512	2300	17:1	{110}<001>
610	2250	15:1	{100}<001>

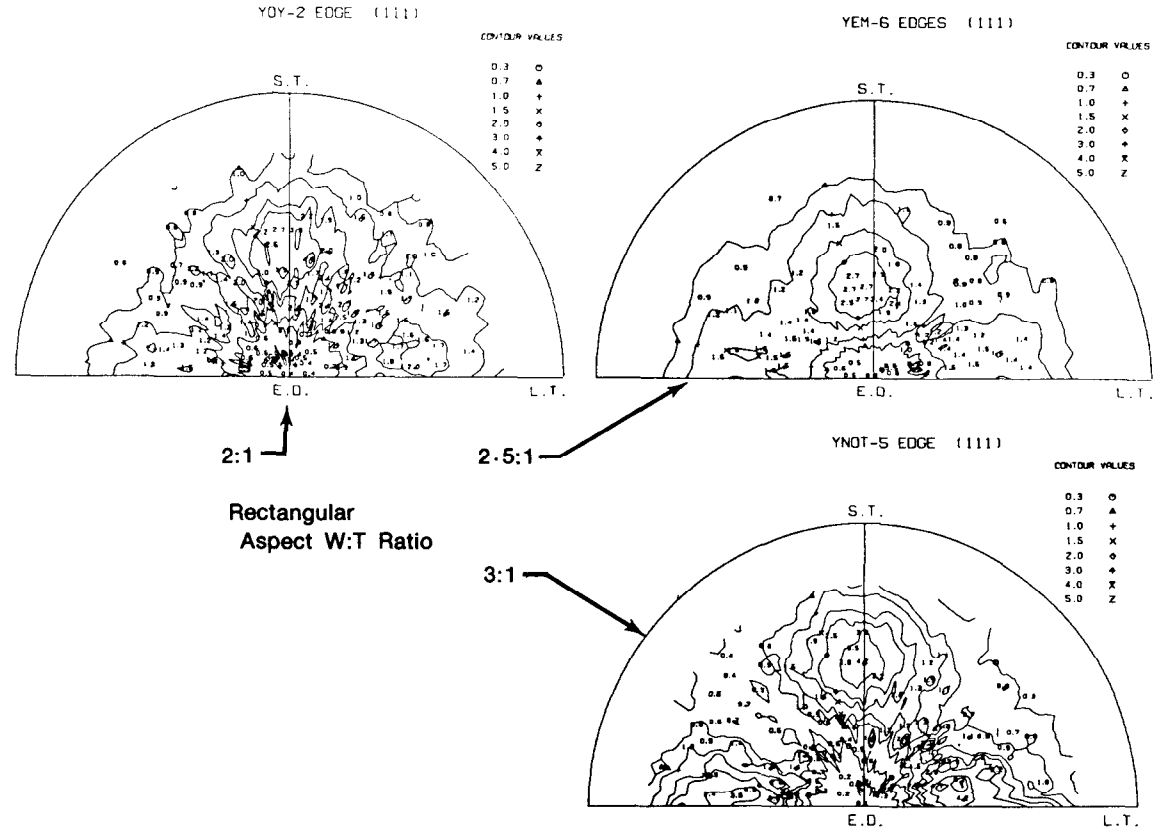

Figure 3. (111) Pole Figures for Rectangular Alloy Y Extrusions of Various Width:Thickness (W:T) Ratios.

Textures developed in Alloy 185 at 2100 to 2300°F exhibited a transition similar to that observed in the round extrusions. The most predominant texture component was the {110}<110> with a weak spread to {100}<011> or {110}<001> end orientations. Alloy 116 extruded at 2300°F exhibited a well defined sheet texture centered about {110}<001>. At lower temperatures, texture spreads were observed {100}<001> to {110}<001> end orientations. With the exception of alloys 607 and 610, the modified

Ni-Mo-Al-X and Ni-Cr-Al-X alloys were observed to develop similar textures to their base compositions for the processing parameters studied; see Table VI for the Ni-Cr-Al-X modified alloys.

For Alloy 607, the Mo and Al additions of Alloy 185 were lowered to 10% and 6.6 % respectively such that the Mo was unsaturated and the γ-γ' phase lattice mismatch was reduced to essentially 0% ($\sim$0.8-1% at RT for Alloy 185). This appeared to have caused a fundamental difference in mode of deformation and resultant texture development. Alloy 607 was observed to develop a {110}<001> textures similar to Ni-Cr-Al-X alloys with 0% γ-γ' mismatch as studied. For Alloy 610, the Cr content of the Ni-Cr-Al-X base was lowered to 5%. This change resulted in the development of a cube texture {100}<001> as compared to the {110}<001> for the base composition. Such behavior is thought to be due to compositional effects on the manner in which deformation and subsequent recrystallization occurs. Meshchaninov and Khayutin (10) reported on the ability to produce the cube texture in several dilute Ni alloys containing Al and Cr. Dillamore and Katoh (11) and Verbraak et. al. (12, 13) rationalized the cube texture development in terms of the alloying effect on the relative mobility of large and small angle boundaries during recrystallization.

Rolling

Hot Rolling. Hot straight rolling was found to impart similar texture components to both Alloys 185 and 116. Both exhibited a texture spread about end orientations {113}<332>and {110}<112>, with the most prominent component at {113}<332>. The texture strengths were weak, typically at 2-3 times random. The texture strength was not significantly affected by deformation temperature, although the Alloy 185 strip rolled at 2000°F (the extreme lower hot rolling workability limit) exhibited 3-4 times random texture strength.

The absence of a temperature-related texture transition in the hot rolled 116 and 185 was thought to be a result of heat losses during rolling. Thus, actual rolling temperatures were lower than for extrusion, and texture transitions were insignificant, as with the lower temperature (<2250°F) extrusions.

The low texture strengths of the hot rolled alloys is thought to be due in part to grain boundary sliding resulting from high temperature and moderate strain rate deformation of these fine grained materials. Such behavior has been observed in superplastically deformed Ni based superalloys (14-16) and aluminum alloys (17).

Cold Rolling. Four different input textures of extruded Alloy 185 and three of extruded Alloy 116 were cold straight rolled. All responded in a similar fashion. Regardless of input texture, both alloys developed a weakly defined FCC sheet type texture with as little as 9% reduction. With increased reduction, the sheet texture increased in definition (i.e. reduced spread) and strength. Textures could be described as a spread about end orientations {113}<332> and {110}<112>. The sheet textures were 2.5 times random at 25% reduction and 4-5 times random at 36% reduction. Reductions greater than 35% resulted in even stronger and better-defined textures.

The deformation texture developed for both alloys was found to be unchanged by the subsolvus (2200°F/5 min/air cool) intermediate annealing treatments used throughout the rolling schedule. Other annealing cycles up to 2300°F yielded similar results. Such behavior has been rationalized as

crystallization in situ, whereby restoration occurs by subgrain rearrangement in the absence of movable recrystallization fronts. This was caused by the strong inhibitive effect of the ordered γ' phase on the growth of the classic fcc {100}<001> annealing texture nuclei (18).

The texture development observed for both alloys appears to follow the trends reported in the literature for other FCC metals and alloys. In the case of Alloys 185 and 116, the end orientation {110}<112> is always present for the range of reductions studied. The major texture component, {113}<332> lies 10° off the {112}<111> by rotation about a <110> and is thought to be a product of the low to intermediate SFE alloys for the specific processing conditions. This is consistent with Dillamore's hypothesis (19) which characterizes the high SFE rolling texture as centered at the {4,4,11}<11,11,8>, this component being a product of cross slip ({113}<332> lies 2° from the {4,4,11}<11,11,8>). Theories for the characteristic plane strain rolling textures have been discussed extensively in the literature (20-25).

Through cross rolling, both Alloys 185 and 116 were observed to develop similar textures. The major effect of cross rolling was to change the straight rolling texture spread into a symmetric singular texture, centered at the {110}<112> component. The degree of textural singularity was observed to be dependent on the ratio of the straight to cross roll reductions, i.e. SR:XR. For Alloys 185 and 116, a fair degree of singularity was achieved using SR:XR ratios within the bounds 80:20 and 60:40. Above and below these bounds the textures more closely matched those of straight rolled product, parallel to and 90° off the original (straight) rolling direction, respectively. Textural singularity also was observed in hot cross rolled product, centered at {110}<112>, although the texture strength was significantly lower. Figure 4 shows pole figures for cold cross rolled Alloy 185. Modified Ni-Mo-Al-X and Ni-Cr-Al-X alloys that were cold rolled, developed textures similar to the base compositions. Figure 4 shows the results for the modified Ni-Mo-Al-X alloys, where the straight roll texture spread {113}<332> to {110}<112> and the singular cross roll texture {110}<112> are observed.

Conclusions

Textures developed in the Ni-Mo-Al-X alloys were typical of moderately high stacking fault energy FCC metals, whilst textures for the Ni-Cr-Al-X alloys were typical of low stacking fault energy alloys. By axisymmetric extrusion at high temperature, the Ni-Mo-Al-X alloys developed a singular <111> fiber texture; the Ni-Cr-Al-X alloys developed a singular <100> fiber texture. At lower extrusion temperatures, the Ni-Mo-Al-X alloys exhibited a texture transition through a narrow triplex <111> + <110> + <100> fiber texture region to a duplex <111> + <100> fiber texture; the Ni-Cr-Al-X alloys exhibited a texture transition to a duplex <111> + <100> fiber texture. Rectangular extrusions bearing width:thickness ratios >2:1 developed sheet type textures; {110}<110> with a weak spread to {110}<001> for Ni-Mo-Al-X alloys, and {110}<001> for Ni-Cr-Al-X alloys. By rolling exclusively in the subsolvus region, texture development was observed to be similar in both classes of alloys. By room temperature rolling, a strong sheet type texture was developed, centered at {113}<332> with spread in ideal orientations to {110}<112> end orientation. In situ recrystallization was observed for intermediate anneal below the alloy's γ' solvus (no texture change). During hot rolling similar textures were observed, though the strength was markedly lower. Cross rolling resulted in preferential development of a singular {110}<112>; the extent of singularity being a function of the straight to cross roll reduction ratio.

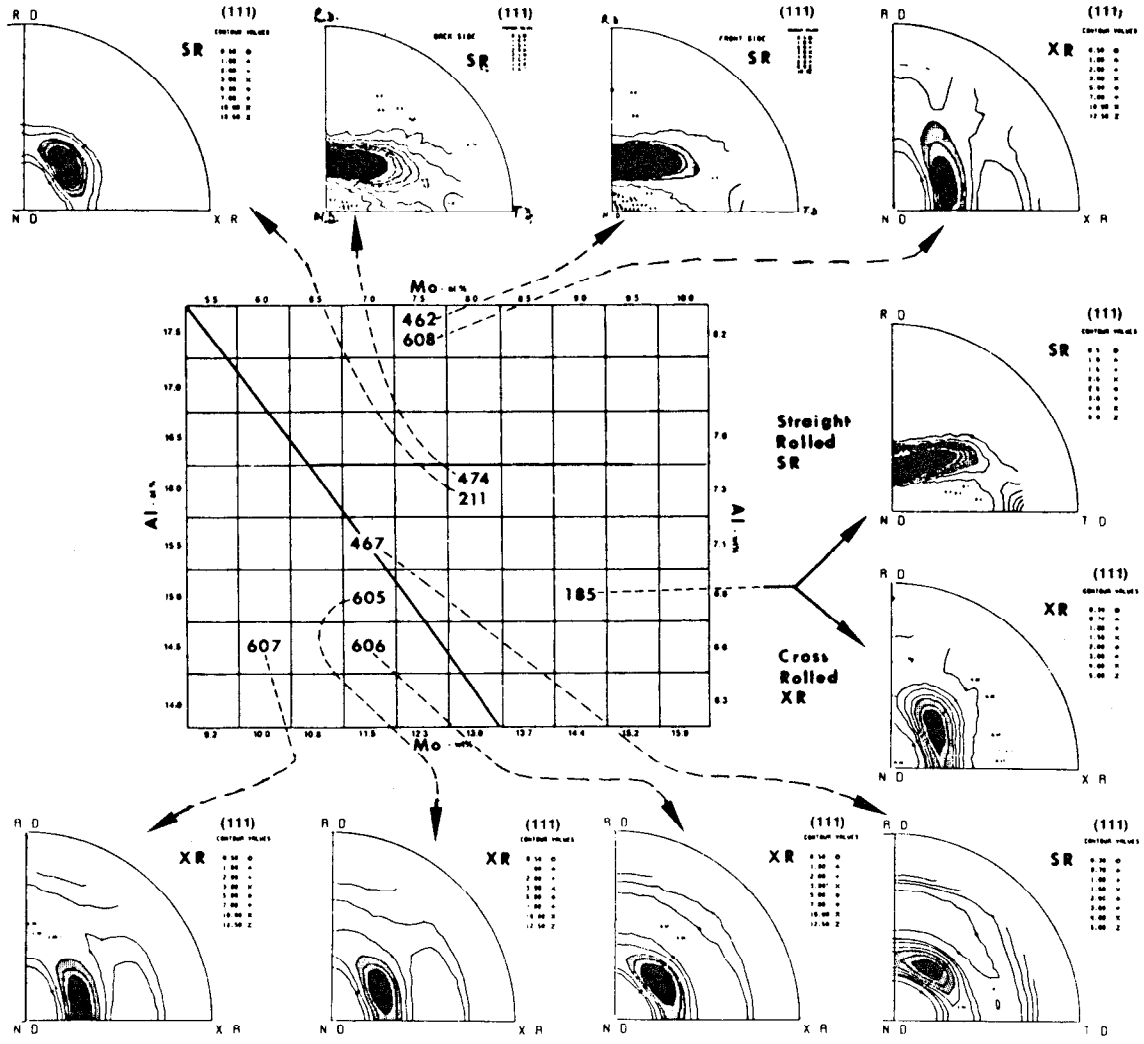

Figure 4. Map of Crystallographic Textures Showing Generic Behavior in Cold Straight or Cross Rolled Ni-Mo-Al-X Alloys.

The development of rolling texture is not significantly affected by initial texture, as beyond 30% reduction that texture is totally eliminated.

Acknowledgements

The authors wish to thank O. B. Cavin (ORNL) and J. Umbach (PWA/GPD) for pole figure generation, J. Zindel for the extrusion studies, J. Andrus for the rolling studies, and R. E. Anderson and J. A. Miller for their constructive discussions and support.

This work is jointly sponsored and monitored by the U. S. Defense Advanced Research Projects Agency and the Air Force Wright Aeronautical Laboratories. The views and conclusions contained in this paper are those of the authors and should not be interpreted as necessarily representing the official policies, either expressed or implied, of the U. S. Defense Research Projects Agency, U. S. Air Force and the U. S. Government.

References

1. A. R. Cox, J. B. Moore and E. C. Van Reuth, Rapidly Solidified Powders, AGARD Conference Proceedings No. 256, 1978.
2. P. R. Holiday, A. R. Cox and R. J. Patterson, II, Proc. Int. Conf. on Rapid Solidification, Reston, VA, Nov. 1977, 245-257.
3. R. E. Anderson, et. al., Proc. Sec. Int. Conf. on Rapid Solidification, Reston, VA, 1980, 416-428.
4. A. R. Cox and R. J. Ondercin, MTAG Conf., Phoenix, AZ, 1979.
5. D. B. George, B. T. Brown and A. R. Cox, AIAA/SAE/ASME 15th Joint Propulsion Conf., Las Vegas, Nevada, 1979.
6. G. R. Love, Oak Ridge National Lab. Tach. Memo, ORNL-TM-2018, 1968.
7. I. L. Dillamore and W. T. Roberts, Met. Review, 1965, Vol. 10, P. 271.
8. H. Hu, Texture, 1974, Vol. 1, p. 233.
9. H. J. McQueen and J. J. Jonas, Treat, Mat. Sci, Tech., Vol. 6, 1975.
10. I. A. Meshchaninov and S. G. Khayutin, Fixika Matallov I Metallovedenie, 42, No. 5, 1976, p. 1029-1033.
11. I. L. Dillamore and H. Katoh, Met. Sci., 1974, Vol. 8, p. 73.
12. C. A. Verbraak, Acto Met., 1958, Vol. 6, p. 280.
13. C. A. Verbaak and W. G. Burgers, Acta Met., 1957, Vol. 5, p. 765.
14. Patent #3, 519, 503 "Fab. Method High Temp. Alloys", July, 1970.
15. R. L. Athey and J. B. Moore, SAE Paper #751047, 1975.
16. H. A. Chin, PWA/GPD Unpublished Work, 1975.
17. R. H. Bricknell and J. W. Edington, Acta Met., 1979, Vol. 27, p. 1303.
18. E. Hornbogen and H. Kreye, Proc. Intl. Symposium on Textures in Research and Practice, Clausthal - Zellerfeld, 1968, p. 274.
19. I. L. Dillamore, Met. Trans. 1970, Vol. 1, p. 2463.
20. H. Mueller, Osterr. Adad. Wiss. Math Naturw. 1958, Vol. 7, p. 117.
21. I. L. Dillamore and W. T. Roberts, ACTA Met., 1964, Vol. 12, p. 281.
22. I. L. Dillamore and H. Katoh, Brit. I. S. Res. Assoc. Rep #MG/39/71, 1971.
23. I. L. Dillamore and H. Katoh, Metal Science, 1974, Vol. 8, p. 21.
24. T. Kamijo, Trans. JIM, 1969, Vol. 10, p. 238.
25. M. Hatherly, and I. L. Dillamore, J. Aust. Inst. Met., 1975, Vol. 20, p. 71.